Modular space-vector pulse-width modulation for nine-switch converters

Dehghan, Seyed Mohammad; Amiri, Arash; Mohamadian, Mustafa; Andersen, Michael A. E.

Published in:
I E T Power Electronics

Link to article, DOI:
10.1049/iet-pel.2012.0203

Publication date:
2013

Citation (APA):
Dehghan, S. M., Amiri, A., Mohamadian, M., & Andersen, M. A. E. (2013). Modular space-vector pulse-width modulation for nine-switch converters. I E T Power Electronics, 6(3), 457-467. DOI: 10.1049/iet-pel.2012.0203

www.ietdl.org

Published in IET Power Electronics
Received on 7th April 2012
Revised on 13th December 2012
Accepted on 22nd December 2012
doi: 10.1049/iet-pel.2012.0203

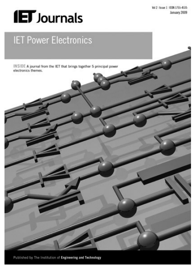

ISSN 1755-4535

Modular space-vector pulse-width modulation for nine-switch converters

Seyed Mohammad Dehghan[1], Arash Amiri[2], Mustafa Mohamadian[2], Michael A.E. Andersen[3]
[1]Faculty of Electrical and Computer Engineering, Qom University of Technology, Qom, Iran
[2]Faculty of Electrical and Computer Engineering, Tarbiat Modares University, Tehran, Iran
[3]Department of Electrical Engineering, Technical University of Denmark, Kongens Lyngby 2800, Denmark
E-mail: dehghan@qut.ac.ir

Abstract: Recently, nine-switch inverter (NSI) has been presented as a dual-output inverter with constant frequency (CF) or different frequency (DF) operation modes. However, the CF mode is more interesting because of its lower switching device rating. This study proposes a new space-vector modulation (SVM) method for the NSI that supports both the CF and DF modes, whereas conventional SVM of NSI can be used only in the DF mode. The proposed SVM can be easily implemented based on the conventional six-switch inverter SVM modules. The performance of the proposed SVM is verified by the simulation and experimental results.

1 Introduction

Over the past few years, there has been an increasing interest in compact, integrated and reduced-component power converters because of their efficiency, volume and cost issues [1–8]. Nine-switch inverter (NSI) is a compact dual-output inverter presented to control two AC loads [9]. The NSI is composed of only nine semiconductor switches (Fig. 1). The NSI has been used for various applications, such as motor control [10], uninterruptible power supply [11, 12], hybrid electric vehicle [13], wind power conversion system [14] and unified power quality conditioner [15]. In addition, some integrated converters have been presented based on the NSI [16–19].

A pulse-width modulation (PWM) method for the NSI has been presented in [9, 10] (Fig. 2). In this method, two (upper and lower) reference signals are used for each phase. By comparing a carrier signal with the upper and lower reference signals, gate signals are generated for upper and lower switches, respectively. The gate signal for mid switch is generated by the logical XOR of the gate signals of the upper and lower switches.

In [11, 12], two operation modes are defined for the NSI, considering the frequencies of the outputs: different frequency (DF) and constant frequency (CF). In the DF mode, two outputs of the inverters have independent frequencies and phases but limited amplitudes. However, in the CF mode, the outputs have same frequency and dependent phases but higher amplitudes. It is obvious from Fig. 2 that in the DF mode, the sum of modulation indices of two outputs must be less than or equal to one; however, the sum of modulation indices can be more than one in the CF mode (it can be as high as 2 for the outputs with the same phase).

The space-vector modulation (SVM) techniques are widely developed and used for power converters [20–23]. A SVM method has been presented for the NSI in [24]. The SVM presented in [24] increases the sum of modulation indices to 1.15 and reduces the number of switching to 2/3 in DF mode. The SVM presented in [24] only supports DF mode.

This paper presents a new SVM for both the DF and CF modes. The SVM proposed in [24] is generalised for all modes in this paper. Also, two practical implementation methods are presented for the proposed SVM.

This paper is organised as follows: Section 2 describes the switching vectors of the NSI. Section 3 presents the proposed SVM methods for the NSI based on the conventional SVM modules. In Section 4, the validity of the proposed method is proved. Section 5 discusses the maximum modulation indices. Finally, Section 6 presents simulation and experimental results.

2 Switching vectors of NSI

Considering three switches in each leg of the NSI, the semiconductors of each leg can have eight different ON–OFF positions. However, to avoid DC bus short-circuit, all three switches cannot be ON at the same time. On the other hand, to avoid floating the connected loads, at least two switches should be ON. Therefore only three ON–OFF positions are possible. Table 1 shows these positions called $\{1\}$, $\{0\}$ and $\{-1\}$. In Table 1, J refers to leg A, B or C; U, M and L refers to the upper, mid and lower semiconductor. Considering three possible states for each leg, there are 27 various states for the NSI. Table 2 shows these states, called NSI vector ($\boldsymbol{V}^N$) in this paper. The NSI vectors can be divided into five groups:

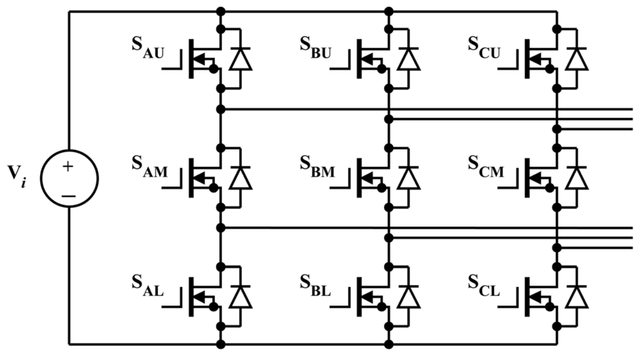

Fig. 1 *Nine-switch inverter*

1. *Zero vectors:* Both the outputs are in a zero state. In the zero state, the load is short-circuited.
2. *Upper-active vectors:* The upper output is in an active state, but the lower output is in a zero state.
3. *Lower-active vectors:* The lower output is in an active state, but the upper output is in a zero state.
4. *Identical-active vectors:* Both the outputs are in a similar active state.
5. *Adjacent-active vectors:* The outputs are in different active states (neighbour active states).

Fig. 3 shows the space presentation and one-switching transfer diagrams of the NSI vectors. In the one-switching transfer diagram, only one switching is required to transfer between two the NSI vectors connected to each other. In Table 2, the vectors have been named considering the state of two outputs. For example, in $V^{N}{}_{01}$, the upper output is in the zero state, but the lower output is in the active vector V_1 (in comparison to a conventional six-switch inverter), or in $V^{N}{}_{21}$, the upper

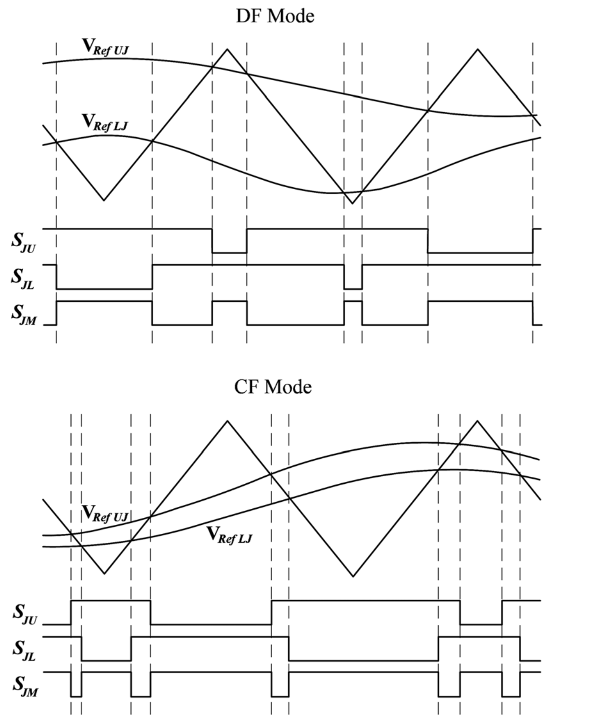

Fig. 2 *Carrier-based PWM method of NSI: DF mode (TOP figure) and CF mode (BOTTOM figure)*

Table 1 Semiconductors ON–OFF position of legs

	1	0	−1
S_{JU}	ON	OFF	ON
S_{JM}	OFF	ON	ON
S_{JL}	ON	ON	OFF

Table 2 Switching vectors of NSI

NSI vector	Leg A	Leg B	Leg C	Type	Equivalent conventional vector	
					Upper	Lower
$V^{N}{}_{ZM}$	1	1	1	zero	V_7	V_0
$V^{N}{}_{ZU}$	0	0	0		V_0	V_0
$V^{N}{}_{ZL}$	−1	−1	−1		V_7	V_7
$V^{N}{}_{10}$	1	0	0	upper-active	V_1	V_0
$V^{N}{}_{20}$	1	1	0		V_2	V_0
$V^{N}{}_{30}$	0	1	0		$^{N}{}_{3}$	V_0
$V^{N}{}_{40}$	0	1	1		V_4	V_0
$V^{N}{}_{50}$	0	0	1		V_5	V_0
$V^{N}{}_{60}$	1	0	1		V_6	V_0
$V^{N}{}_{01}$	−1	1	1	lower-active	V_7	V_1
$V^{N}{}_{02}$	−1	−1	1		V_7	V_2
$V^{N}{}_{03}$	1	−1	1		V_7	V_3
$V^{N}{}_{04}$	1	−1	−1		V_7	V_4
$V^{N}{}_{05}$	1	1	−1		V_7	V_5
$V^{N}{}_{06}$	−1	1	−1		V_7	V_6
$V^{N}{}_{11}$	−1	0	0	identical-active	V_1	V_1
$V^{N}{}_{22}$	−1	−1	0		V_2	V_2
$V^{N}{}_{33}$	0	−1	0		V_3	V_3
$V^{N}{}_{44}$	0	−1	−1		V_4	V_4
$V^{N}{}_{55}$	0	0	−1		V_5	V_5
$V^{N}{}_{66}$	−1	0	−1		V_6	V_6
$V^{N}{}_{21}$	−1	1	0	adjacent-active	V_2	V_1
$V^{N}{}_{23}$	1	−1	0		V_2	V_3
$V^{N}{}_{43}$	0	−1	1		V_4	V_3
$V^{N}{}_{45}$	0	1	−1		V_4	V_5
$V^{N}{}_{65}$	1	0	−1		V_6	V_5
$V^{N}{}_{61}$	−1	0	1		V_6	V_1

doi: 10.1049/iet-pel.2012.0203

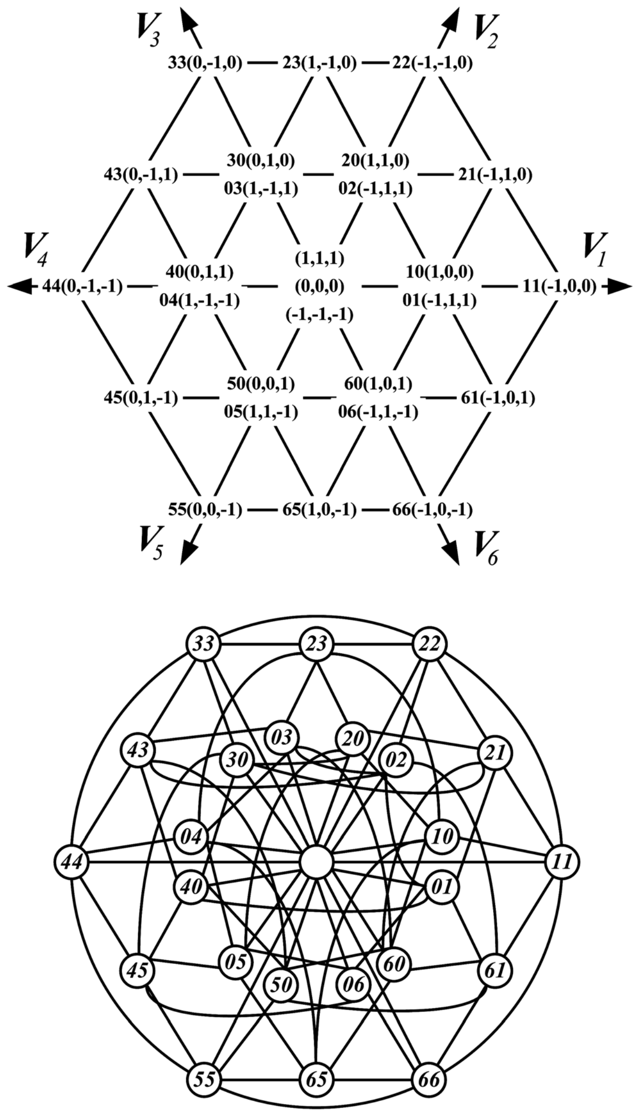

Fig. 3 *Switching vectors of NSI: space diagram presentation (TOP figure) and transfer diagram between vectors with one switching (BOTTOM figure)*

output has the conventional vector V_2, but the lower output is in the vector V_1. Zero vectors are named $V^N{}_{\text{ZM}}$, $V^N{}_{\text{ZU}}$ and digital signal processor $V^N{}_{\text{ZL}}$. Only the middle switches in $V^N{}_{\text{ZM}}$, the upper switches in $V^N{}_{\text{ZU}}$ and the lower switches in $V^N{}_{\text{ZL}}$ are OFF.

3 Proposed SVM for NSI

Fig. 4 shows the proposed SVM for the NSI. In the proposed method, two synchronised SVM modules of conventional six-switch inverter are used. The SVM modules have different voltage references $\left(\bar{V}_{\text{ref } U} \text{and} \bar{V}_{\text{ref } L}\right)$ related to the upper and lower outputs, respectively. Twelve switching pulses generated by two SVM modules are used to produce nine switching pulses, which are required for NSI as shown in Fig. 4. Considering the dead time for each SVM, the required dead time for NSI is automatically generated.

In the proposed method, to avoid interference of the active vectors of the upper and lower SVMs, different vector placement patterns should be used for each SVM modules.

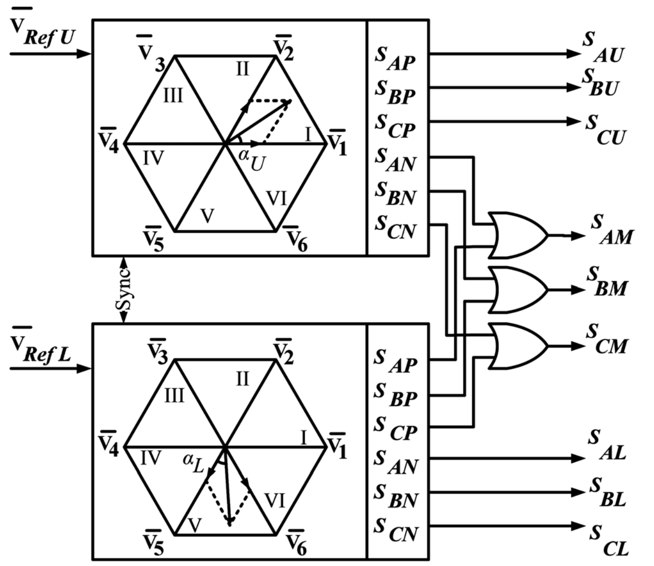

Fig. 4 *Proposed modular SVM for NSI*

Fig. 5 (upper figure) shows a proposed placement method for a typical state when the upper reference signal is in sector 1 and the lower reference signal is in sector 2. In this method, the conventional zero vectors V_0 and V_7 are removed from the upper and lower SVMs, respectively. In other words, the active vectors of the upper and lower SVM are shifted to the left and right, respectively. Therefore, we call this method 'shifting method'. It can be found from Figs. 4 and 5 that combination of the vectors of two SVM modules generates two NSI upper-active vectors, one NSI zero vector and two NSI lower-active vectors. When the sum of modulation indices of two SVM modules is greater than 1.15 (CF mode), NSI identical-active and adjunct-active vectors may be added to switching cycle (Fig. 5, middle figure). It can be proved that if a CF mode (with given modulation index and phase) is feasible, all NSI vectors generated by the proposed method will be practical (Table 2 shows practical NSI vectors). In Section 5, conditions of feasible CF mode is survived.

In the shifting method, because of the placement of the active vectors in the corner of the switching cycle, the total harmonic distortion (THD) is high. The vectors V_0 and V_7

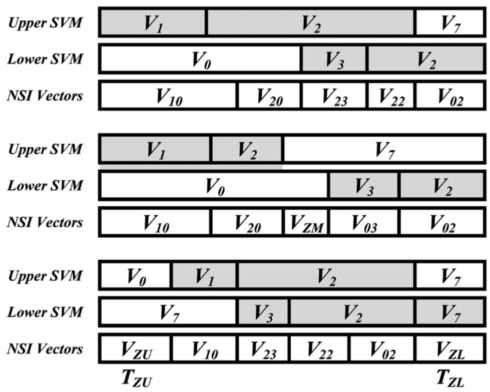

Fig. 5 *Vector-placement methods*

(TOP to BOTTOM): Shifting method in DF mode, shifting method in CF mode, and ZVT method

doi: 10.1049/iet-pel.2012.0203

Table 3 Time interval of zero vectors (ZVT method)

Type	(R_U, R_L)	Condition	T_{0max}
same sector	(1,1),(3,3),(5,5)	$T_1 + T_2 > T_3 + T_4$ & $T_2 > T_4$	$T - T_1 - T_2$
		$T_1 + T_2 < T_3 + T_4$ & $T_3 > T_1$	$T - T_3 - T_4$
		Else	$T - T_1 - T_4$
	(2,2),(4,4),(6,6)	$T_1 + T_2 > T_3 + T_4$ & $T_1 > T_3$	$T - T_1 - T_2$
		$T_1 + T_2 < T_3 + T_4$ & $T_4 > T_2$	$T - T_3 - T_4$
		Else	$T - T_2 - T_3$
neighbour sectors	(1,2),(3,4),(5,6)	$T_2 > T_3 + T_4$	$T - T_1 - T_2$
		$T_2 < T_3 + T_4$	$T - T_1 - T_3 - T_4$
	(2,3),(4,5),(6,1)	$T_3 > T_1 + T_2$	$T - T_3 - T_4$
		$T_3 < T_1 + T_2$	$T - T_1 - T_2 - T_4$
	(2,1),(4,3),(6,5)	$T_1 > T_3 + T_4$	$T - T_1 - T_2$
		$T_1 < T_3 + T_4$	$T - T_2 - T_3 - T_4$
	(3,2),(5,4),(1,6)	$T_4 > T_1 + T_2$	$T - T_3 - T_4$
		$T_4 < T_1 + T_2$	$T - T_1 - T_2 - T_3$
far sectors	(1,3),(3,5),(5,1)	$T_2 > T_3$	$T - T_1 - T_2 - T_4$
		$T_2 < T_3$	$T - T_1 - T_3 - T_4$
	(2,4),(4,6),(6,2) (3,1),(5,3),(1,5)	–	$T - T_1 - T_2 - T_3 - T_4$
	(4,2),(6,4),(2,6)	$T_1 > T_4$	$T - T_1 - T_2 - T_3$
		$T_1 < T_4$	$T - T_2 - T_3 - T_4$
	$(R, R \pm 2)$	–	$T - T_1 - T_2 - T_3 - T_4$

with the time intervals T_{ZU} and T_{ZL} can be added to the upper and lower SVMs, respectively, as shown in Fig. 5 (lower figure). It can be proved that if the sum of T_{ZU} and T_{ZL} is less than a maximum zero time interval (T_{0max}), the resulting NSI vectors are still practical (T_{0max} is determined by Table 3). Adding the mentioned zero vectors shifts the active vectors of both the SVMs to the centre of the switching cycle, and consequently, THD decreases. This method needs a table of the maximum time intervals for the zero vectors, and the authors named it, zero vector table (ZVT) method. In Table 3, T_1 and T_2 are the time intervals of the upper SVM active vectors and T_3 and T_4 are the time intervals of the lower SVM active vectors. These time intervals are calculated by

$$T_1 = \frac{\sqrt{3}}{2} m_U T \sin\left(\frac{\pi}{3} - \alpha_U\right) \tag{1}$$

$$T_2 = \frac{\sqrt{3}}{2} m_U T \sin(\alpha_U) \tag{2}$$

$$T_3 = \frac{\sqrt{3}}{2} m_L T \sin\left(\frac{\pi}{3} - \alpha_L\right) \tag{3}$$

$$T_4 = \frac{\sqrt{3}}{2} m_L T \sin(\alpha_L) \tag{4}$$

where T is the switching period. m_U and m_L are the upper and lower modulation indices respectively. α_U and α_L are upper and lower phases, respectively. In both the ZVT and shifting methods, Table 3 can be used to investigate permissible modulation indices. If value T_{0max} is negative, it means that the selected modulation indices cannot be implemented.

4 Proof of proposed SVM method

In this section, first a method is proposed to determine the NSI vectors directly, and then the optimum NSI vectors selection procedure is described. Finally, the ZVT and shifting modular SVM methods are derived from the optimum direct SVM method.

4.1 Direct SVM method

The location of the reference signals in the space diagram determines the required conventional vectors for the switching. For example, if the upper reference signal is in the sector 1 and the lower reference signal is in the sector 2, the upper output needs the conventional vectors V_1 and V_2 and the lower output needs V_2 and V_3. For the implementation of these conventional vectors, the equivalent NSI vectors should be selected. For example, the NSI vectors $\boldsymbol{V}^N{}_{10}$, $\boldsymbol{V}^N{}_{20}$, $\boldsymbol{V}^N{}_{02}$, $\boldsymbol{V}^N{}_{03}$, $\boldsymbol{V}^N{}_{22}$ and $\boldsymbol{V}^N{}_{23}$ can be used. The desirable time interval (even zero) can be chosen for each of these NSI vectors, while the time intervals T_1, T_2, T_3 and T_4 [(1)–(4)] should be satisfied. For this example, we have

$$\begin{aligned} T_1 &= T_{10} \\ T_2 &= T_{20} + T_{22} + T_{23} \\ T_3 &= T_{02} + T_{22} \\ T_4 &= T_{03} + T_{23} \end{aligned} \tag{5}$$

where T_{10}, T_{20}, T_{02}, T_{03}, T_{22} and T_{23} are time intervals of the NSI vectors $\boldsymbol{V}^N{}_{10}$, $\boldsymbol{V}^N{}_{20}$, $\boldsymbol{V}^N{}_{02}$, $\boldsymbol{V}^N{}_{03}$, $\boldsymbol{V}^N{}_{22}$ and $\boldsymbol{V}^N{}_{23}$, respectively. It is obvious that using the identical-active and adjunct-active vectors can reduce the required time, and this especially can be used for the CF mode. In the rest of the switching period, the zero vectors ($\boldsymbol{V}^N{}_{ZM}$, $\boldsymbol{V}^N{}_{ZU}$ and $\boldsymbol{V}^N{}_{ZL}$) should be used. The time intervals of the zero vectors are desirable, and they should satisfy following equation

$$T_0 = T_{ZM} + T_{ZU} + T_{ZL} \tag{6}$$

where T_0 is the total time interval of the zero vectors and T_{ZM}, T_{ZU} and T_{ZL} are time intervals of the NSI vectors $\boldsymbol{V}^N{}_{ZM}$, $\boldsymbol{V}^N{}_{ZU}$ and $\boldsymbol{V}^N{}_{ZL}$, respectively.

4.2 Optimum direct SVM method

As described already, various combinations of the NSI vectors can be selected for a given condition. In an optimum NSI vector sequence, using identical-active and adjunct-active vectors have priority over than upper-active and lower-active vectors. Also, in an optimum sequence, the number of switching should be the minimum. For this purpose, the one-switching transfer diagram (Fig. 3) can be used. An optimum sequence should make a continuous path in the one-switching transfer diagram.

The selection of the optimum sequence is depended on the position of the reference signals in the space diagram. The position of the reference signals has three possible conditions as follows:

Same sectors: For the CF mode, only when the phase difference between the references is less than 60°, the references can be placed in the same sector. In this situation, both active vectors can be used to reduce the total

doi: 10.1049/iet-pel.2012.0203

required time interval. For example, when $R_U = R_L = 1$ and $T_2 > T_3 + T_4$, the sequence $\{V^N_{ZU}, V^N_{10}, V^N_{20}, V^N_{21}, V^N_{22}, V^N_{ZL}\}$ with the time intervals $\{T_{ZU}, T_1, T_2–T_3–T_4, T_3, T_4, T_{ZL}\}$ is recommended.

Neighbour sectors: For the CF mode, only when the phase difference between the references is less than 120°, the references are placed in the neighbour sectors. In all sequences for this situation, an adjunct-active vector and in some sequences an identical-active vector can be used to reduce the total required time interval. For example, when $R_U = 3$, $R_L = 4$ and $T_2 > T_3 + T_4$, the sequence $\{V^N_{ZU}, V^N_{30}, V^N_{40}, V^N_{45}, V^N_{44}, V^N_{ZL}\}$ with the time intervals $\{T_{ZU}, T_1, T_2–T_3–T_4, T_4, T_3, T_{ZL}\}$ is recommended.

Far sectors: When the reference signals are placed in two far sectors, the identical-active vectors cannot used at all. When the difference between sectors is two, using the adjunct-active vectors might be possible. However, it cannot reduce the total time interval, because it is not available in all over the fundamental period. For example, when $R_U = 3$, $R_L = 5$ and $T_2 > T_3$, the sequence $\{V^N_{ZU}, V^N_{30}, V^N_{40}, V^N_{45}, V^N_{06}, V^N_{ZL}\}$ with the time intervals $\{T_{ZU}, T_1, T_2–T_3, T_3, T_4, T_{ZL}\}$ is recommended.

A table of the optimum sequences can be produced for various conditions. In all the suggested sequences $T_0 = T_{ZU} + T_{ZL}$. It is possible to choose $T_{ZU} = 0$ or $T_{ZL} = 0$, in such a manner that one of the vectors is removed, and consequently, the switching number reduces. However, if we select $T_{ZU} = T_{ZL} = T_0/2$, the output THD is reduced.

4.3 Modular SVM methods

ZVT method: As described, all the optimum sequences can be divided into two groups of the conventional vectors. For example, when $R_U = 1$ and $R_L = 2$, the sequence $\{V^N_{ZU}, V^N_{10}, V^N_{23}, V^N_{22}, V^N_{02}, V^N_{ZL}\}$ with the time intervals $\{T_{ZU}, T_1, T_4, T_2–T_4, T_3 + T_4–T_2, T_{ZL}\}$ may occur. This sequence offers the conventional vectors $\{V_0, V_1, V_2, V_7\}$ with $\{T_{ZU}, T_1, T_2, T_3 + T_4–T_2 + T_{ZL}\}$ for the upper output and $\{V_0, V_3, V_2, V_7\}$ with $\{T_{ZU} + T_1, T_4, T_3, T_{ZL}\}$ for the lower output. The important point is the time intervals of zero vectors. In fact, two outputs act as two independent inverters. Only the time intervals of the zero vectors are dependent on each other. Actually, the time intervals are $\{T_{ZU}, T_1, T_2, T–T_1–T_2 + T_{ZU}\}$ and $\{T–T_3–T_4–T_{ZL}, T_4, T_3, T_{ZL}\}$ for the upper and lower outputs, respectively. It means by using the information about T_{ZL} and T_{ZU}, the SVM for each output can be implemented independently and separately. This can be implemented using a table of the time intervals of the zero vectors for different conditions (Table 3).

Shifting method: As described, an NSI sequence can be divided into two upper and lower groups (Fig. 5). It is possible that the upper group is shifted to the left (the conventional vector V_0 is removed) and the lower group is shifted to the right (without V_7) (Fig. 5). It can be proved that new sequences are also possible. In new sequences, the upper and lower groups are quite independent (even in the time interval of the zero vectors). Shifting sequences can be implemented for all recommended sequences. The shifting method does not change the switching number and the optimum use of the time interval. In the shifting method, V^N_{ZU} and V^N_{ZL} are removed and V^N_{ZM} may be inserted to the sequence. Although the shifting method uses two fully independent SVMs, the output THD is more than the ZVT method.

5 Maximum modulation indices

The maximum modulation indices for various conditions are calculated in this section. The sum of the time intervals of the active NSI vectors (T_{SA}) when the reference signals are in the same sector can be calculated by

$$\begin{aligned} T_{SA} = \max\left[m_1 \sin\left(60 - \alpha_U\right), m_2 \sin\left(60 - \alpha_L\right)\right] \\ + \max\left[m_1 \sin\left(\alpha_U\right), m_2 \sin\left(\alpha_L\right)\right] \end{aligned} \tag{7}$$

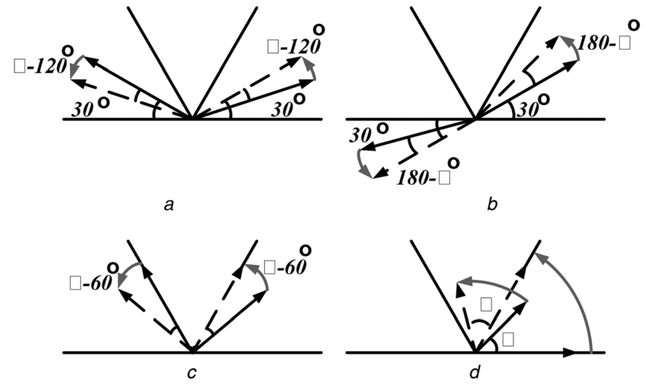

Fig. 6 *Maximum required time interval for reference signals, with phase difference*
a 120–150
b 150–180
c 60–120
d 0–60

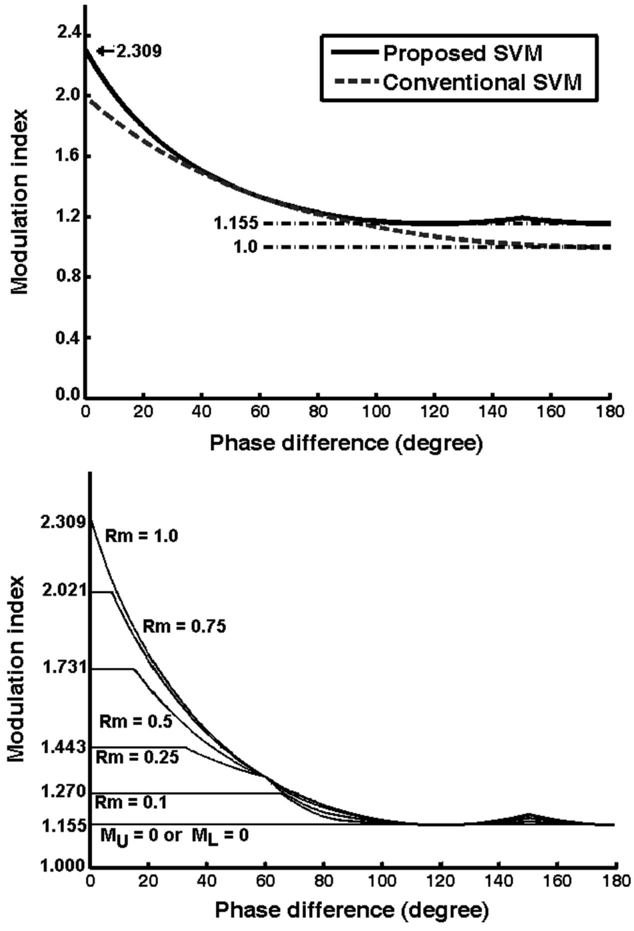

Fig. 7 *Maximum sum modulation indices for: $R_m = 1$ (top figure) and various R_m (bottom figure)*

doi: 10.1049/iet-pel.2012.0203

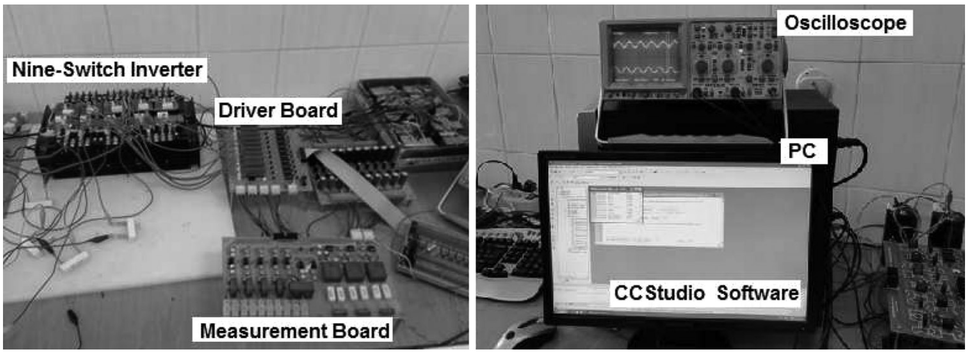

Fig. 8 *Experimental set-up of NSI*

When the reference signals are in two neighbour sectors, and the upper reference is ahead of the lower reference, T_{SA} is equal to one of the following equations depending on the sectors

$$\begin{aligned} &\text{Upper Sector} = \text{Even, Lower Sector} = \text{Odd:} \\ &\quad T_{SA} = m_1 \sin(\alpha_U) + \max\big[m_1 \sin(60 - \alpha_U), \\ &\quad\quad m_2 \sin(60 - \alpha_L) + m_2 \sin(\alpha_L)\big] \\ &\text{Upper Sector} = \text{Odd, Lower Sector} = \text{Even} \\ &\quad T_{SA} = m_2 \sin(60 - \alpha_L) + \max\big[m_2 \sin(\alpha_L), \\ &\quad\quad m_1 \sin(60 - \alpha_U) + m_1 \sin(\alpha_U)\big] \end{aligned} \tag{8}$$

When the reference signals are in two neighbour sectors, and the lower reference is ahead of the upper reference, T_{SA} is equal to one of the following equations depending on the sectors

$$\begin{aligned} &\text{Upper Sector} = \text{Even, Lower Sector} = \text{Odd} \\ &\quad T_{SA} = m_1 \sin(60 - \alpha_U) + \max\big[m_1 \sin(\alpha_U), \\ &\quad\quad m_2 \sin(60 - \alpha_L) + m_2 \sin(\alpha_L)\big] \\ &\text{Upper Sector} = \text{Odd, Lower Sector} = \text{Even} \\ &\quad T_{SA} = m_2 \sin(\alpha_L) + \max\big[m_2 \sin(60 - \alpha_L), \\ &\quad\quad m_1 \sin(60 - \alpha_U) + m_1 \sin(\alpha_U)\big] \end{aligned} \tag{9}$$

Finally, when the reference signals are at two far sectors, T_{SA} can be expressed by

$$\begin{aligned} T_{SA} = {} & m_1 \sin(60 - \alpha_U) + m_1 \sin(\alpha_U) \\ & + m_2 \sin(60 - \alpha_L) + m_2 \sin(\alpha_L) \end{aligned} \tag{10}$$

When the phase difference between the reference signals (θ) is greater than 120°, the reference signals are always in two far sectors. Therefore the identical and adjunct-active vectors are not useful. Figs. 6*a* and *b* show the worst condition for $120° < \theta < 150°$ and $150° < \theta < 180°$, respectively. In these figures, the sum of the time intervals of one of the references is increasing to the maximum and the other one is decreasing from the maximum. The maximum sum of the time intervals of the active NSI vectors ($T_{SA\text{-}MAX}$) occurs in the shown areas. For $m_U = m_L = m$, from (10), it can be proved that

$$m = \frac{2}{\sqrt{3}\cos(\theta/2) + 3\sin(\theta/2)}, \quad 120^\circ \le \theta \le 150^\circ \tag{11}$$

$$m = \frac{1}{\sqrt{3}\sin(\theta/2)}, \quad 150^\circ \le \theta \le 180^\circ \tag{12}$$

For $60° < \theta < 120°$, the reference signals are either in the neighbour sectors or in the far sectors. Obviously, $T_{SA\text{-}MAX}$ occurs when the reference signals are placed in two far sectors (Fig. 6*c*). For $m_U = m_L = m$, it can be proved that

$$m = \frac{2}{\sqrt{3}\cos(\theta/2) + 3\sin(\theta/2)}, \quad 60^\circ \le \theta \le 120^\circ \tag{13}$$

When the phase difference between the reference signals is less than 60°, the reference signals are either in the same sector or in two neighbour sectors (Fig. 6*d*). However, considering (7)–(9), $T_{SA\text{-}MAX}$ can only occur in one of these states. For $m_U = m_L = m$, it can be proved that $T_{SA\text{-}MAX}$ occurs when the signals are at same sector and is equal to

$$m = \frac{1}{\sqrt{3}\sin(\theta/2 + 30)}, \quad 0^\circ \le \theta \le 60^\circ \tag{14}$$

Fig. 7 (top figure) shows the maximum modulation index when $m_U = m_L$ for the proposed SVM and conventional PWM. It can be seen that except for $\theta = 60°$, the proposed SVM increases the maximum modulation index. The maximum modulation index of the conventional PWM for

Table 4 Simulation and experimental parameters

Parameter	Value
switching frequency	3 kH
deadtime	3 uS
R_{load}	5.6 Ohm
L_f	1.5 mH
C_f	15 uF
Vdc	150 V
m_U	1
m_L	0.5
f_U	50 Hz
f_L	50 Hz
θ ($\alpha_U = 0$, $\alpha_U = \theta$)	25°

doi: 10.1049/iet-pel.2012.0203

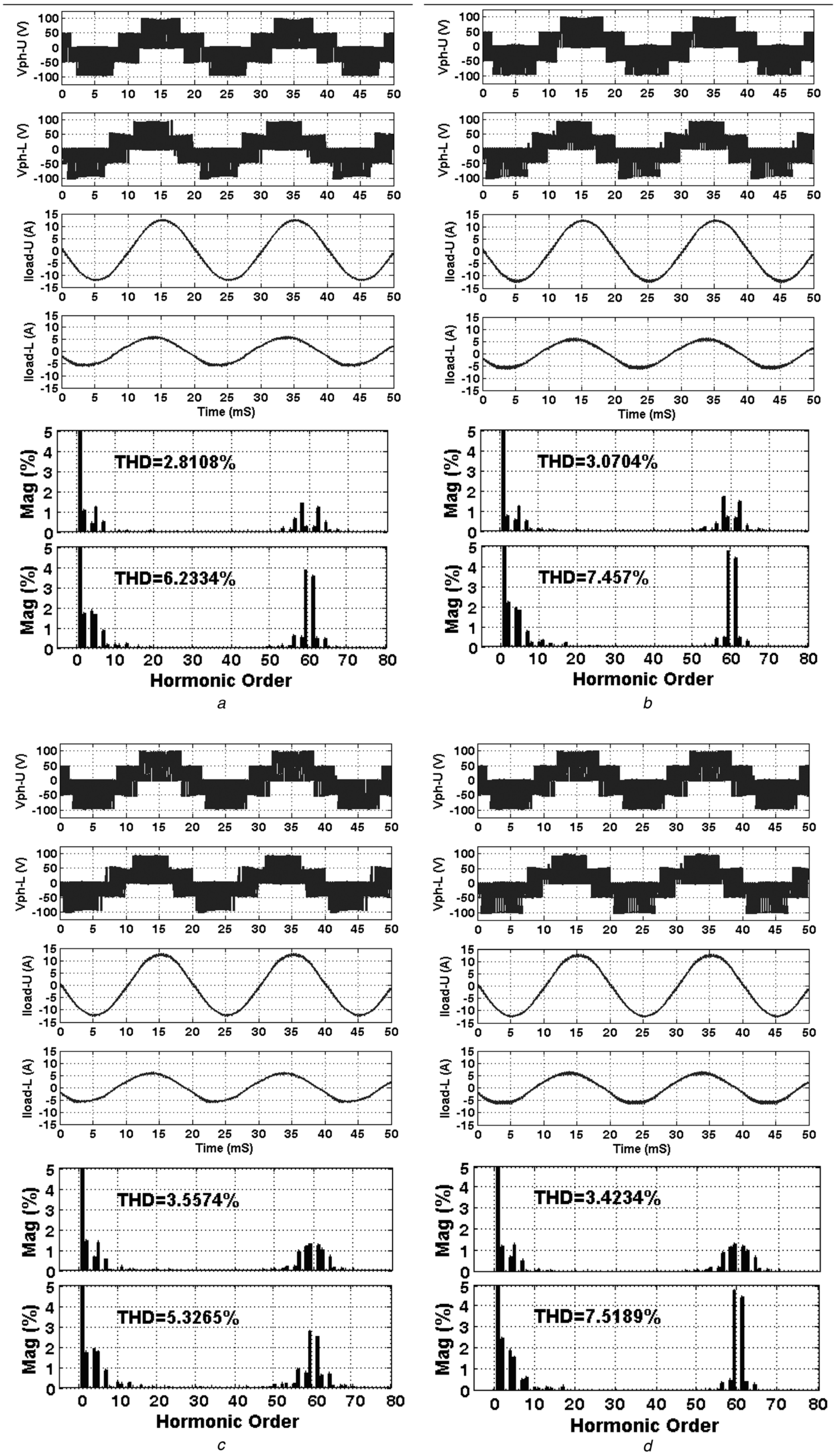

Fig. 9 *Simulation results in CF mode for*

a ZVT method with $T_{ZU} = T_{ZL}$
b ZVT method with $T_{ZL} = 0$
c ZVT method with $T_{ZU} = 0$
d Shifting method (TOP to BOTTOM): Upper phase voltage, lower phase voltage, upper load current, lower load current, frequency spectra of upper current and frequency spectra of lower currents

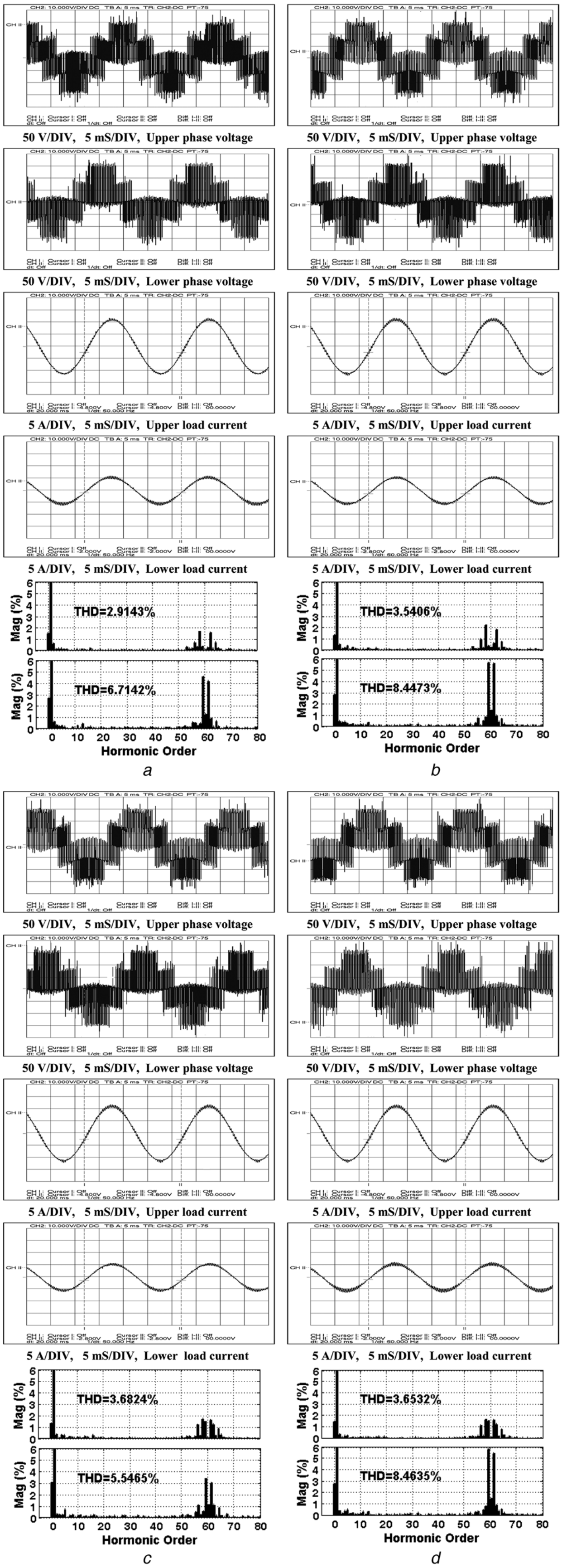

Fig. 10 *Experimental results in CF mode*

a ZVT method with $T_{ZU} = T_{ZL}$
b ZVT method with $T_{ZL} = 0$
c ZVT method with $T_{ZU} = 0$
d Shifting method (TOP to BOTTOM): Upper phase voltage, lower phase voltage, upper load current, lower load current, frequency spectra of upper current and frequency spectra of lower currents

$m_U = m_L$ can be calculated as [25]

$$m = \frac{1}{1 + \sin(\theta/2)}, \quad 0^\circ \le \theta \le 180^\circ \tag{15}$$

Fig. 7 (bottom figure) shows the maximum sum of modulation indices for various ratios between the modulation indices ($m_U = m_L \; R_m$ or $m_L = m_U \; R_m$). The maximum sum of modulation indices, when the phase difference is zero can be calculated as $1.15(1 + R_m)$.

6 Simulations and experimental results

In this section, the performance and the validity of the proposed SVMs are investigated by the computer simulation and experimental prototype (Fig. 8). A laboratory prototype of the NSI was implemented using nine IXYS60N120D1 switches and was controlled using TMS320F2812 digital signal processor (DSP). For both the simulation and experimental verifications, two similar resistive loads with LC filters are connected to the outputs of inverter. Table 4 shows the simulation and experimental parameters.

For comparison and analysis, various SVMs were applied to NSI: (i) ZVT method with $T_{ZU} = T_{ZL}$, (ii) ZVT method with $T_{ZL} = 0$, (iii) ZVT method with $T_{ZU} = 0$ and (iv) Shifting method. Figs. 9 and 10 show the simulation and experimental results for these four methods. It can be seen that the NSI outputs are satisfactory in all the methods. Table 5 shows the THD and frequency spectra of load currents of the NSI for various methods. As expected, the shifting method offers the worst THD. The ZVT method with $T_{ZU} = 0$ has the lowest THD for the lower output. Since the lower output has smaller modulation index, with $T_{ZU} = 0$, the active vectors of the lower output are shifted to the centre of the switching cycle and this leads to the improved THD. Since the upper output has larger modulation index, in the ZVT method with $T_{ZU} = T_{ZL}$, its active vectors are placed almost at the centre. Therefore with $T_{ZL} = 0$ or $T_{ZU} = 0$, the upper output THD increases. For various modulation indices and phase differences, a specific combination of T_{ZL} and T_{ZU} gives the best THD performance for the upper or lower output. It can be seen that there is a close match between the simulation and experimental results.

7 Conclusions

In this paper, a new SVM for the NSI was proposed. The proposed SVM can be used in both the constant frequency (CF) and different frequency (DF) modes, whereas the former SVM method only supports the DF mode. In the proposed method, five types of the switching vectors are defined for the NSI: zero, upper-active, lower-active, identical-active and adjunct-active vectors. Since during the identical-active and adjunct-active vectors, both the outputs are in the active state, these vectors are useful for the CF mode. Based on the proposed SVM, two different methods were proposed to control the outputs independently in both the CF and DF modes (ZVT method and shifting method). The performance of the proposed SVMs was verified using the simulation and experimental results.

doi: 10.1049/iet-pel.2012.0203

Table 5 THD of load currents for various SVM methods

Method	Upper output		Lower output	
	Simulation, %	Experimental, %	Simulation, %	Experimental, %
ZVT method with $T_{ZU} = T_Z$	2.81	2.91	6.23	6.71
ZVT method with $T_{ZL} = 0$	3.07	3.54	7.45	8.41
ZVT method with $T_{ZU} = 0$	3.56	3.68	5.32	5.54
shifting method	3.42	3.65	7.51	8.46

8 References

1 Mondal, G., Gopakumar, K., Tekwani, P.N., Levi, E.: 'A reduced-switch-count five-level inverter with common-mode voltage elimination for an open-end winding induction motor drive', *IEEE Trans. Ind. Electron.*, 2007, **54**, (4), pp. 2344–2351
2 Jones, M., Vukosavic, S.N., Dujic, D., Levi, E., Wright, P.: 'Five-leg inverter PWM technique for reduced switch count two-motor constant power applications', *IET Electr. Power Appl.*, 2008, **2**, (5), pp. 275–287
3 Lezana, P., Rodriguez, J., Oyarzun, D.A.: 'Cascaded multilevel inverter with regeneration capability and reduced number of switches', *IEEE Trans. Ind. Electron.*, 2008, **55**, (3), pp. 1059–1066
4 Itoh, J., Noge, Y., Adachi, T.: 'A novel five-level three-phase PWM rectifier with reduced switch count', *IEEE Trans. Power Electron.*, 2011, **26**, (8), pp. 2221–2228
5 dos Santos, E.C., Jacobina, C.B., de Almeida Carlos, G.A., de Freitas, I. S.: 'Component minimized AC–DC–AC single-phase to three-phase four-wire converters', *IEEE Trans. Ind. Electron.*, 2011, **58**, (10), pp. 4624–4635
6 Ebrahimi, J., Babaei, E., Gharehpetian, G.B.: 'A new multilevel converter topology with reduced number of power electronic components', *IEEE Trans. Ind. Electron.*, 2012, **59**, (2), pp. 655–667
7 Chu, G.M.L., Lu, D.D.C., Agelidis, V.G.: 'Flyback-based high step-up converter with reduced power processing stages', *IET Power Electron.*, 2012, **5**, (3), pp. 349–357
8 Figarado, S., Bhattacharya, T., Mondal, G., Gopakumar, K.: 'Three-level inverter scheme with reduced power device count for an induction motor drive with common-mode voltage elimination', *IET Power Electron.*, 2008, **1**, (1), pp. 84–92
9 Kominami, T., Fujimoto, Y.: 'A novel nine-switch inverter for independent control of two three-phase loads'. IEEE Industry Applications Society Annual Conference (IAS), 2007, pp. 2346–2350
10 Kominami, T., Fujimoto, Y.: 'Inverter with reduced switching-device count for independent ac motor control'. Proc. IEEE-IECON'07, 2007, pp. 1559–1564
11 Liu, C., Wu, B., Zargari, N., Xu, D.: 'A novel three-phase three-leg AC/AC converter using nine IGBTs', *IEEE Trans. Power Electron.*, 2009, **24**, (5), pp. 1151–1160
12 Liu, C., Wu, B., Zargari, N., Xu, D.: 'A novel nine-switch PWM rectifier-inverter topology for three-phase UPS applications', *J. Eur. Power Electron. (EPE)*, 2009, **19**, (2), pp. 1–10
13 Dehghan, S.M., Mohamadian, M., Yazdian, A.: 'Hybrid electric vehicle based on bidirectional Z-source nine-switch inverter', *IEEE Trans. Veh. Technol.*, 2010, **59**, (6), pp. 2641–2653
14 Astad, K.P., Molinas, M.: 'Direct AC/AC power converter for wind power application'. 15th IEEE Mediterranean Electrotechnical Conf. (MELECON2010), Valletta, Malta, 2010, pp. 113–118
15 Zhang, L., Loh, P.C., Gao, F.: 'An integrated nine-switch power conditioner'. Int. Power Electronics Conf. (IPEC2010), Sapporo, Japan, 2010, pp. 2663–2669
16 Azizi, M., Fatemi, A., Mohamadian, M., Yazdian, A.: 'A novel Z-source four-leg inverter with two independent four-wire outputs'. Power Electronic & Drive Systems & Technologies Conf. (PEDSTC2010), Tehran, Iran, 2010, pp. 163–168
17 Dehghan, S.M., Mohamadian, M., Yazdian, A., Ashrafzadeh, F.: 'A dual-input dual-output Z-source inverter', *IEEE Trans. Power Electron.*, 2010, **25**, (2), pp. 360–368
18 Dehghan, S.M., Mohamadian, M., Yazdian, A., Rajaei, A.H., Zahedi, H.: 'Dual Z-source network dual-input dual-output inverter', *Iranian J. Electr. Electron. Engng. (IJEEE)*, 2010, **6**, (4), pp. 205–213
19 Liu, X., Wang, P., Loh, P.C., Blaabjerg, F.: 'A compact three-phase single-input/dual-output matrix converter', *IEEE Trans. Ind. Electron.*, 2012, **59**, (1), pp. 6–16
20 Saeedifard, M., Iravani, R., Pou, J.: 'Control and DC-capacitor voltage balancing of a space vector-modulated five-level STATCOM', *IET Power Electron.*, 2009, **2**, (3), pp. 203–215
21 Rabinovici, R., Baimel, D., Tomasik, J., Zuckerberger, A.: 'Series space vector modulation for multi-level cascaded H-bridge inverters', *IET Power Electron.*, 2010, **3**, (6), pp. 843–847
22 Adam, G.P., Finney, S.J., Ojo, O., Williams, B.W.: 'Quasi-two-level and three-level operation of a diode-clamped multilevel inverter using space vector modulation', *IET Power Electron.*, 2012, **5**, (5), pp. 542–552
23 Patkar, F., Levi, E., Jones, M.: 'A six-phase multilevel space vector PWM algorithm for a dual-inverter supplied drive'. IET Int. Conf. on Power Electronics, Machines and Drives (PEMD), University of Bristol, UK, 2012
24 Dehghan, S.M., Mohamadian, M., Yazdian, A., Ashrafzadeh, F.: 'Space vectors modulation for nine-switch converters', *IEEE Trans. Power Electron.*, 2010, **25**, (9), pp. 1488–1496
25 Gao, F., Zhang, L., Li, D., Loh, P.C., Tang, Y., Gao, H.: 'Optimal pulse-width modulation of nine-switch converter', *IEEE Trans. Power Electron.*, 2010, **25**, (9), pp. 2331–2343

9 Appendix

In regard to Section 4.2 of paper, *Optimum Direct SVM Method*, Tables 6–8 show all recommended optimum sequences for various conditions.

Table 6 Recommended sequences of NSI vectors when references signals are at same sector

Conditions	Vectors			Time intervals	T_0
	$R_U = R_L = 1$	$R_U = R_L = 3$	$R_U = R_L = 5$		
$T_1 + T_2 > T_3 + T_4$ $T_2 > T_3 + T_4$	ZU,10,20,21,22, ZL	ZU,30,40,43,44, ZL	ZU,50,60,65,66, ZL	T_{ZU}, T_1, $T_2 - T_3 - T_4$, T_3, T_4, T_{ZL}	$T - T_1 - T_2$
$T_1 + T_2 > T_3 + T_4$ $T_4 < T_2 < T_3 + T_4$	ZU,10,11,21,22, ZL	ZU,30,33,43,44, ZL	ZU,50,55,65,66, ZL	T_{ZU}, $T_1 + T_2 - T_3 - T_4$, $T_3 + T_4 - T_2$, $T_2 - T_4$, T_4, T_{ZL}	$T - T_1 - T_2$
$T_1 + T_2 > T_3 + T_4$ $T_2 < T_4$	ZU,10,11,22,02, ZL	ZU,30,33,44,04, ZL	ZU,50,55,66,06, ZL	T_{ZU}, $T_1 - T_3$, T_3, T_2, $T_4 - T_2$, T_{ZL}	$T - T_1 - T_4$
$T_1 + T_2 < T_3 + T_4$ $T_3 > T_1 + T_2$	ZU,11,21,01,02, ZL	ZU,33,43,03,04, ZL	ZU,55,65,05,06, ZL	T_{ZU}, T_1, T_2, $T_3 - T_1 - T_2$, T_4, T_{ZL}	$T - T_3 - T_4$
$T_1 + T_2 < T_3 + T_4$ $T_1 < T_3 < T_1 + T_2$	ZU,11,21,22,02, ZL	ZU,33,43,44,04, ZL	ZU,55,65,66,06, ZL	T_{ZU}, T_1, $T_3 - T_1$, $T_1 + T_2 - T_3$, $T_3 + T_4 - T_1 - T_2$, T_{ZL}	$T - T_3 - T_4$
$T_1 + T_2 < T_3 + T_4$ $T_3 < T_1$	ZU,10,11,22,02, ZL	ZU,30,33,44,04, ZL	ZU,50,55,66,06, ZL	T_{ZU}, $T_1 - T_3$, T_3, T_2, $T_4 - T_2$, T_{ZL}	$T - T_1 - T_4$
	$R_U = R_L = 2$	$R_U = R_L = 4$	$R_U = R_L = 6$		
$T_1 + T_2 > T_3 + T_4$ $T_1 > T_3 + T_4$	ZU,30,20,23,22, ZL	ZU,50,40,45,44, ZL	ZU,10,60,61,66, ZL	T_{ZU}, T_2, $T_1 - T_3 - T_4$, T_4, T_3, T_{ZL}	$T - T_1 - T_2$
$T_1 + T_2 > T_3 + T_4$ $T_3 < T_1 < T_3 + T_4$	ZU,30,33,23,22, ZL	ZU,50,55,45,44, ZL	ZU,10,11,61,66, ZL	T_{ZU}, $T_1 + T_2 - T_3 - T_4$, $T_3 + T_4 - T_1$, $T_1 - T_3$, T_3, T_{ZL}	$T - T_1 - T_2$
$T_1 + T_2 > T_3 + T_4$ $T_1 < T_3$	ZU,30,33,22,02, ZL	ZU,50,55,44,04, ZL	ZU,10,11,66,06, ZL	T_{ZU}, $T_2 - T_4$, T_4, T_1, $T_3 - T_1$, T_{ZL}	$T - T_2 - T_3$
$T_1 + T_2 < T_3 + T_4$ $T_4 > T_1 + T_2$	ZU,33,23,03,02, ZL	ZU,55,45,05,04, ZL	ZU,11,61,01,06, ZL	T_{ZU}, T_2, T_1, $T_4 - T_1 - T_2$, T_3, T_{ZL}	$T - T_3 - T_4$
$T_1 + T_2 < T_3 + T_4$ $T_2 < T_4 < T_1 + T_2$	ZU,33,23,22,02, ZL	ZU,55,45,44,04, ZL	ZU,11,61,66,06, ZL	T_{ZU}, T_2, $T_4 - T_2$, $T_1 + T_2 - T_4$, $T_3 + T_4 - T_1 - T_2$, T_{ZL}	$T - T_3 - T_4$
$T_1 + T_2 < T_3 + T_4$ $T_4 < T_2$	ZU,30,33,22,02, ZL	ZU,50,55,44,04, ZL	ZU,10,11,66,06, ZL	T_{ZU}, $T_2 - T_4$, T_4, T_1, $T_3 - T_1$, T_{ZL}	$T - T_2 - T_3$

Table 7 Recommended sequences of NSI vectors when references signals are at neighbour sectors

Conditions	Vectors			Time interval	T_0
	$R_U = 1$, $R_L = 2$	$R_U = 3$, $R_L = 4$	$R_U = 5$, $R_L = 6$		
$T_2 > T_3 + T_4$	ZU,10,20,23,22,ZL	ZU,30,40,45,44,ZL	ZU,50,60,61,66,ZL	T_{ZU}, T_1, $T_2 - T_3 - T_4$, T_4, T_3, T_{ZL}	$T - T_1 - T_2$
$T_2 > T_4$	ZU,10,23,22,02,ZL	ZU,30,45,44,04,ZL	ZU,50,61,66,06,ZL	T_{ZU}, T_1, T_4, $T_2 - T_4$, $T_3 + T_4 - T_2$, T_{ZL}	$T - T_1 - T_3 - T_4$
$T_2 < T_4$	ZU,10,23,03,02,ZL	ZU,30,45,05,04,ZL	ZU,50,61,01,06,ZL	T_{ZU}, T_1, T_2, $T_4 - T_2$, T_3, T_{ZL}	$T - T_1 - T_3 - T_4$
	$R_U = 2$, $R_L = 3$	$R_U = 4$, $R_L = 5$	$R_U = 6$, $R_L = 1$		
$T_3 > T_1 + T_2$	ZU,33,23,03,04,ZL	ZU,55,45,05,06,ZL	ZU,11,61,01,02,ZL	T_{ZU}, T_2, T_1, $T_3 - T_1 - T_2$, T_4, T_{ZL}	$T - T_3 - T_4$
$T_3 > T_1$	ZU,30,33,23,04,ZL	ZU,50,55,45,06,ZL	ZU,10,11,61,02,ZL	T_{ZU}, $T_1 + T_2 - T_3$, $T_3 - T_1$, T_1, T_4, T_{ZL}	$T - T_1 - T_2 - T_4$
$T_3 < T_1$	ZU,30,20,23,04,ZL	ZU,50,40,45,06,ZL	ZU,10,60,61,02,ZL	T_{ZU}, T_2, $T_1 - T_3$, T_3, T_4, T_{ZL}	$T - T_1 - T_2 - T_4$
	$R_U = 2$, $R_L = 1$	$R_U = 4$, $R_L = 3$	$R_U = 6$, $R_L = 5$		
$T_1 > T_3 + T_4$	ZU,30,20,21,22,ZL	ZU,50,40,43,44,ZL	ZU,10,60,65,66,ZL	T_{ZU}, T_2, $T_1 - T_3 - T_4$, T_3, T_4, T_{ZL}	$T - T_1 - T_2$
$T_1 > T_3$	ZU,30,21,22,02,ZL	ZU,50,43,44,04,ZL	ZU,10,65,66,06,ZL	T_{ZU}, T_2, T_3, $T_1 - T_3$, $T_3 + T_4 - T_1$, T_{ZL}	$T - T_2 - T_3 - T_4$
$T_1 < T_3$	ZU,30,21,01,02,ZL	ZU,50,43,03,04,ZL	ZU,10,65,05,06,ZL	T_{ZU}, T_2, T_1, $T_3 - T_1$, T_4, T_{ZL}	$T - T_2 - T_3 - T_4$
	$R_U = 3$, $R_L = 2$	$R_U = 5$, $R_L = 4$	$R_U = 1$, $R_L = 6$		
$T_4 > T_1 + T_2$	ZU,33,43,03,02,ZL	ZU,55,65,05,04,ZL	ZU,11,21,01,06,ZL	T_{ZU}, T_1, T_2, $T_4 - T_1 - T_2$, T_3, T_{ZL}	$T - T_3 - T_4$
$T_4 > T_2$	ZU,30,33,43,02,ZL	ZU,50,55,65,04,ZL	ZU,10,11,21,06,ZL	T_{ZU}, $T_1 + T_2 - T_4$, $T_4 - T_2$, T_2, T_3, T_{ZL}	$T - T_1 - T_2 - T_3$
$T_4 < T_2$	ZU,30,40,43,02,ZL	ZU,50,60,65,04,ZL	ZU,10,20,21,06,ZL	T_{ZU}, T_1, $T_2 - T_4$, T_4, T_3, T_{ZL}	$T - T_1 - T_2 - T_3$

doi: 10.1049/iet-pel.2012.0203

Table 8 Recommended sequences of NSI vectors when references signals are at far sector

Conditions	Vectors			Time interval	T_0
	$R_U = 1$, $R_L = 3$	$R_U = 3$, $R_L = 5$	$R_U = 5$, $R_L = 1$		
$T_2 > T_3$	ZU,10,20,23,04,ZL	ZU,30,40,45,06, ZL	ZU,50,60,61,02, ZL	T_{ZU}, T_1, T_2–T_3, T_3, T_4, T_{ZL}	T–T_1–T_2–T_4
$T_2 < T_3$	ZU,10,23,03,04,ZL	ZU,30,45,05,06, ZL	ZU,50,61,01,02, ZL	T_{ZU}, T_1, T_2, T_3–T_2, T_4, T_{ZL}	T–T_1–T_3–T_4
	$R_U = 2$, $R_L = 4$	$R_U = 4$, $R_L = 6$	$R_U = 6$, $R_L = 2$		
–	ZU,30,20,05,04, ZL	ZU,50,40,01,06, ZL	ZU,10,60,03,02,ZL	T_{ZU}, T_2, T_1, T_4, T_3, T_{ZL}	T–T_1–T_2–T_3–T_4
	$R_U = 3$, $R_L = 1$	$R_U = 5$, $R_L = 3$	$R_U = 1$, $R_L = 5$		
–	ZU,30,40,01,02, ZL	ZU,50,60,03,04, ZL	ZU,10,20,05,06, ZL	T_{ZU}, T_1, T_2, T_3, T_4, T_{ZL}	T–T_1–T_2–T_3–T_4
	$R_U = 4$, $R_L = 2$	$R_U = 6$, $R_L = 4$	$R_U = 2$, $R_L = 6$		
$T_1 > T_4$	ZU,50,40,43,02, ZL	ZU,10,60,65,04, ZL	ZU,30,20,21,06, ZL	T_{ZU}, T_2, T_1–T_4, T_4, T_3, T_{ZL}	T–T_1–T_2–T_3
$T_1 < T_4$	ZU,50,43,03,02, ZL	ZU,10,65,05,04, ZL	ZU,30,21,01,06, ZL	T_{ZU}, T_2, T_1, T_4–T_1, T_3, T_{ZL}	T–T_2–T_3–T_4
	$R_U = 1$, $R_L = 4$	$R_U = 3$, $R_L = 6$	$R_U = 5$, $R_L = 2$		
–	ZU,10,20,05,04, ZL	ZU,30,40,01,06, ZL	ZU,50,60,03,02, ZL	T_{ZU}, T_1, T_2, T_4, T_3, T_{ZL}	T–T_1–T_2–T_3–T_4
	$R_U = 2$, $R_L = 5$	$R_U = 4$, $R_L = 1$	$R_U = 6$, $R_L = 3$		
–	ZU,30,20,05,06 ZL	ZU,50,40,01,02, ZL	ZU,10,60,03,04, ZL	T_{ZU}, T_2, T_1, T_3, T_4, T_{ZL}	T–T_1–T_2–T_3–T_4